Radiocarbon, Vol 65, Nr 4, 2023, p 819–831 DOI:10.1017/RDC.2023.68

$^{14}CO_2$ ACTIVITY IN AIR SAMPLES AND DILUTION FACTOR EVALUATION OF KAKRAPAR GUJARAT SITE, INDIA

A Chandrakar[1]* • A K Patra[1] • C P Joshi[1] • A Jain[1] • D P Nankar[1] • D Badhai[2] • S Karthik[2] • I V Saradhi[3] • A V Kumar[3]

[1]Environmental Survey Laboratory (ESS, EMAD, BARC), Kakrapar Gujarat Site, P.O. Anumala, Surat District, Gujarat-394651, India
[2]Health Physics Unit, KAPS-1&2, Kakrapar Gujarat Site, P.O. Anumala, Surat District, Gujarat-394651, India
[3]Environmental Monitoring and Assessment Division (EMAD), BARC, Mumbai-400 085, India

ABSTRACT. $^{14}CO_2$ activity in air samples collected at Kakrapar Gujarat Site, India, was measured, and site-specific dilution factor for $^{14}CO_2$ has been evaluated. $^{14}CO_2$ activity in air samples was monitored for 72 different sampling events at onsite stack of Nuclear Power Plant (NPP) and at ESL meteorology laboratory (at 1.6 km from NPP stack). $^{14}CO_2$ activity in air at stack of NPP and at ESL meteorology laboratory was observed to 0.10–0.18 TBq $(GW_e.year)^{-1}$, with mean value 0.12 TBq $(GW_e.year)^{-1}$ and ≤0.04–0.13 Bq m^{-3}, with mean value 0.08 Bq m^{-3} respectively. The results were correlated with meteorological parameters. Site specific dilution factor for $^{14}CO_2$ in air was evaluated at 1.6 km and was found to be in the range of 4.6E-05 to 21E-05 s m^{-3}. Inter angle (degree) between plume direction and fixed sampling location and rainfall (mm) are found to be the important influencing parameters for dilution factor of $^{14}CO_2$ in air.

KEYWORDS: ^{14}C, $^{14}CO_2$, dilution factor, Gaussian plume dispersion model (GPM), inter angle, Kakrapar, nuclear power plant (NPP), PHWR.

INTRODUCTION

Radiocarbon (^{14}C) is present in the environment from three sources: natural production (cosmogenic interaction of ^{14}N in upper atmosphere), release from atmospheric tests, and routine release from nuclear installations. ^{14}C is a low energy beta emitter (E_{max}: 156 kev and E_{avg}: 49.5 kev) with long radioactive half-life: 5700 ± 30 yr (Kutschera 2013). ^{14}C is produced in the atmosphere by a variety of reactions, the most important being between thermalized neutrons from cosmic radiation and nitrogen atoms (Davis et al. 1977). The annual cosmogenic production rate of ^{14}C by this process is 1.4×10^6 GBq, and the total inventory of ^{14}C in the atmosphere was estimated to be 1.4×10^8 GBq (IAEA 2004). It has been estimated that a total of 2.2×10^8 GBq ^{14}C was released to the atmosphere by nuclear weapon testing, causing a significantly increased concentration of ^{14}C in the atmosphere in 1950–1960 (IAEA 2004). It has been estimated that about 1.1×10^6 GBq of ^{14}C is produced yearly in the nuclear power plants all over the world, in which about 1.1×10^5 GBq is released to the atmosphere as gaseous form from all operating nuclear power plants and about 3.7×10^5 GBq in both gaseous and liquid forms is released from the reprocessing plants (UNSCEAR 2000). The production rate and pathway of ^{14}C in the nuclear power plants vary with the type of power plants, the concentrations of oxygen and nitrogen in the fuel, structural materials, moderator, and coolant.

^{14}C is an important radionuclide for reactors using heavy water because of larger production than the pressurized water reactor (PWR) and boiling water reactor (BWR) (Graven et al. 2011). ^{14}C production is more in moderator (Joshi et al. 1987; Peterson et al. 1997). The reasons behind higher ^{14}C production and emission in a pressurized heavy water reactor (PHWR) compared to a light water reactor (PWR, BWR) are as follows: (a) average thermal neutron flux in PHWR is higher than LWR, so a large amount of D_2O is present in high thermal neutron fluxes at PHWR, because of this large inventory of ^{17}O arises; and (b) isotopic abundance of ^{17}O in D_2O used in PHWR is higher than in H_2O at LWR (Sohn et al. 2012).

*Corresponding author. Email: amolchandrakar@npcil.co.in

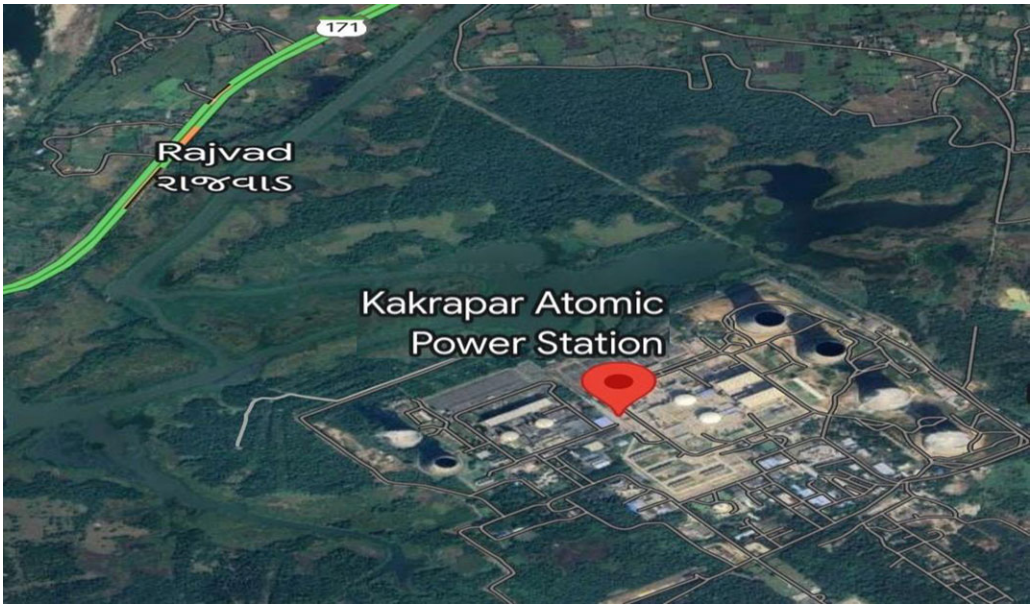

Figure 1A Satellite map around Kakrapar Atomic Power Station.

In PHWR, the majority of ^{14}C releases in the form of $^{14}CO_2$ through the stack (Robertson et al. 1978). It is reported that ^{14}C-free fossil carbon added to atmospheric CO_2 by combustion dilutes the atmospheric $^{14}C/^{12}C$ ratio. However, releases of ^{14}C from nuclear power plants may affect this dilution and may bias $^{14}C/^{12}C$ based estimates of fossil-fuel-derived CO_2 if these nuclear influences are not correctly accounted for (Graven et al. 2011; Lassey et al. 2007a, 2007b). $^{14}CO_2$ in air in the vicinity of a nuclear power plant thus becomes important to be monitored, to check % rise of natural background level, if any (Vokal et al. 1997; Stenström et al. 1998; Molnár et al. 2007; Povinec et al. 2008, 2009; Dias et al. 2009).

Considering the significance, a systematic study on the measurement of $^{14}CO_2$ activity in air at NPP stack (onsite) and at micrometeorological laboratory of Environmental Survey Laboratory (ESL) (at 1.6 km from NPP stack) was carried out, correlated with various meteorological parameters are presented in this paper.

MATERIALS AND METHODS

Site Description and Study Area

This study was carried out at Kakrapar Gujarat nuclear power plant site, situated on the southern bank of Moticher Lake, which is about 85 km by road from Surat city, in the southern region of Gujarat State (latitude 21°14'N; longitude 73°22'E) (Figure 1A). The Kakrapar Gujarat site is comprised of two nuclear power reactors (PHWR type) with a capacity of 220 MWe each (KAPS-1&2). Unit-1 of the power station started commercial operation in May 1993 and Unit-2 in September 1995. One common 100-m-high stack is for both reactors (Kakrapar Atomic Power Station-1&2). Samplings were carried out at the reactor stack (onsite) and at the ESL meteorology laboratory (1.6 km away from the reactor in the NNE downwind sector) (Figure 1B). Both reactors: Unit-1 and Unit-2 were operated in 100% during

https://doi.org/10.1017/RDC.2023.68 Published online by Cambridge University Press

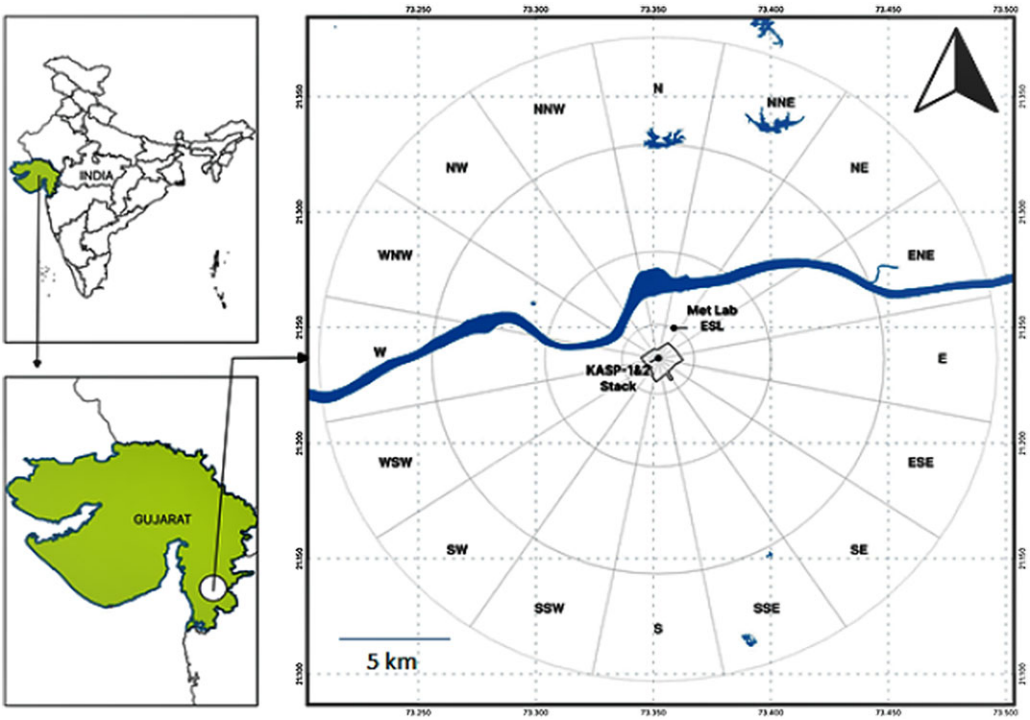

Figure 1B Environmental monitoring map along with sampling locations.

our sampling event. Meteorological parameters such as wind speed, wind direction, ambient temperature, relative humidity, atmospheric pressure, solar radiation, and rainfall are measured at the micrometeorological laboratory of ESL, Kakrapar Gujarat Site. Statistical correlation between the dilution factor of $^{14}CO_2$ at 1.6 km (NNE sector) with influencing meteorological parameters were studied for 72 different sampling events, and correlation coefficient (r) and p value (two-tailed) are tabulated in Table 3.

Air Sample Collection and Processing

Some portion of the effluent gas from the exhaust air of KAPS-1&2 stack was sampled at a rate of 2 lpm and passed through 200 mL of 1M NaOH solution for one hour duration. Simultaneously, $^{14}CO_2$ in air was collected at ESL meteorology laboratory and absorbed in 20 mL of 1M NaOH solution at 2 lpm for 1-hr duration using handheld air sampler (Figure 2). The experiment was conducted during 23/06/2021 to 31/08/2021, and 72 samples were collected from each location. The samples were processed as per standard procedure (Joshi et al. 1987; Baburajan et al. 2020). The Na_2CO_3 generated in the sample was precipitated as $BaCO_3$ by externally adding 20% $BaCl_2$ solution and then centrifuged. $BaCO_3$ precipitate was washed twice by using 40% alcohol in distilled water, and dried under an IR lamp. A known quantity of precipitate was introduced in the acidification setup (Figure 3). 1–2 mL of aqueous solution (88%) of lactic acid is added into dried precipitate of $BaCO_3$. Evolution of CO_2 from $BaCO_3$ is reabsorbed in ethanol amine and methanol (1:4 V/V) absorbing mixture of 10 mL. This was kept overnight. 10 mL of Ultima gold LLT cocktail was added to this mixture, properly

https://doi.org/10.1017/RDC.2023.68 Published online by Cambridge University Press

Figure 2 Handheld air sampler used for bubbling air sample through NaOH solution.

homogenized and then counted for ^{14}C in an ultra-low background liquid scintillation spectrometer (LSS) (Model: Quantulus-1220 by Perkin Elmer).

Methodology for Calculating $^{14}CO_2$ Activity and Uncertainty in the Analysis

$^{14}CO_2$ activity in air sample was calculated using the standard Equation (1) (Baburajan et al. 2020)

$$A = \frac{\text{Net CPM}}{(60*E*V*F*R*Q)} \pm \frac{\sqrt{\frac{SC}{Ts}+\frac{BC}{Tb}}}{(60*E*V*F*R*Q)} \quad (1)$$

Where A: $^{14}CO_2$ activity in Bq m^{-3}. Net CPM = SC – BC (SC: sample CPM, BC: background CPM of chemical blank).

https://doi.org/10.1017/RDC.2023.68 Published online by Cambridge University Press

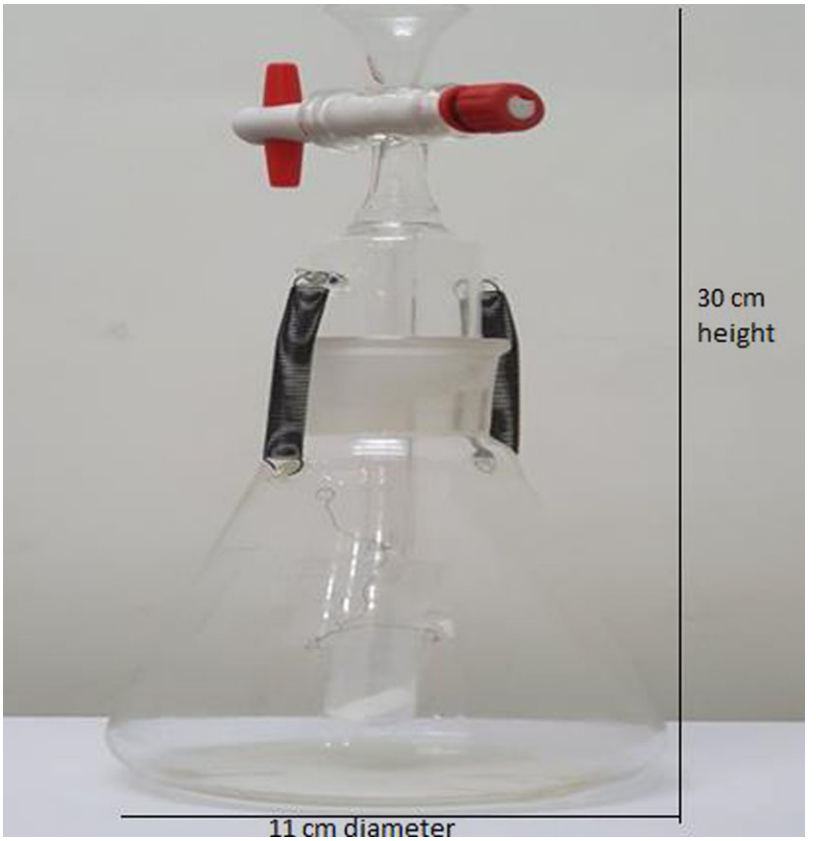

Figure 3 Acidification setup for regeneration of $^{14}CO_2$ absorbed in the organic solvent.

Volume of air sampled (V) in $m^3 = 0.12$.

E: LSS counting efficiency in fraction, which is 0.75 or 75% in our system (using ^{14}C standard spiked to ethanol amine-methanol absorbing mixture). Region of interest in channel (ROI: 130-340) was decided such that figure of merit comes more than 4000 in LSS.

F: fraction of CO_2 absorption in NaOH solution at single stage of impinger/bubbler.

Based on the four set of experiments carried out, mean F value for stack and environmental samplings were found to be 0.44 ± 0.03 and 0.56 ± 0.024, respectively.

R: recovery factor (analytical yield calculated from first step: precipitation of $BaCO_3$ to last step: reabsorbed CO_2 in absorbing mixture), known inorganic form ^{14}C activities of following: 14.79, 29.58, 44.37, 59.16, and 73.95 Bq spiked to 1M NaOH solutions of 200 mL (for stack sample) and 20 mL (for environmental sample). Recovery factor was calculated from ^{14}C spiked activity and ^{14}C recovered activity. Mean recovery factor of five set of data was found to be 0.80 ± 0.06 and 0.82 ± 0.07 for stack and environmental sample, respectively.

Q: Fraction of $BaCO_3$ which is introduced in acidification setup wrt total $BaCO_3$ yield, ≤ 1.

https://doi.org/10.1017/RDC.2023.68 Published online by Cambridge University Press

Ts and Tb: LSS operating time in minutes of sample and background, respectively. In our case Ts = Tb.

Overall uncertainty (U) of the mentioned procedure for $^{14}CO_2$ measurement in air sample was computed using Equation (2) (IAEA-TECDOC-1401 2004; Baburajan et al. 2020).

$$U = \sqrt{(U_1)^2 + (U_2)^2 + (U_3)^2 + (U_4)^2 + (U_5)^2} \tag{2}$$

Sources of relative uncertainties are U_1 to U_5.

U_1: Sampling uncertainty in % (by taking single stage bubbler)

U_2: Weighing ($BaCO_3$ precipitate) uncertainty in %

U_3: Recovery factor uncertainty in %

U_4: LSS efficiency calibration uncertainty in %

U_5: LSS count rate uncertainty in %

Each uncertainty component was quantified. U_1 and U_3 were calculated by using coefficient of variation in %. For stack (200 mL) and environmental sampling (20 mL), U_1 were 6.81% and 4.28%, respectively and U_3 were 7.50% and 8.53%, respectively. U_2 was 0.1% as per the manufacture certification of our electronic weighing balance. U_4 was 1.3%. U_5 is based on Equation (3) (Huang et al. 2015).

$$U_5 = \frac{\sqrt{\frac{SC}{Ts} + \frac{BC}{Tb}}}{SC - BC} * 100 \tag{3}$$

In order to detect low level of activity, counting time is increased which reduces counting uncertainty. For environmental sample (Ts = Tb = 1440 min) and stack sample (Ts = Tb = 60 min), the calculated U_5 is 8.25% and 2.45%, respectively.

By putting the value of all relative uncertainties in equation 2, overall uncertainty (U) was found to be 13% and 11% for environmental and stack sample, respectively.

Minimum Detectable Level (MDL) of ^{14}C in Air

MDL of ^{14}C in air Bq m^{-3} at a confidence level of 99.7% is calculated as per Equation (4);

$$MDL = \frac{3 * \sqrt{\frac{BC}{T}}}{60 * E * V * F * R * Q} \tag{4}$$

For Quantulus-1220 LSS, BC = 1.07 CPM; T = 1440 minutes; counting efficiency (E) = 75%, Uncertainty in MDL is calculated by using error propagation. Since environmental data are reported at 95% confidence level, the uncertainty corrected MDL value is 0.032 ± 0.008Bq m^{-3}, varies from 0.024 to 0.04Bq m^{-3}. By taking upper limit, MDL is considered as 0.04Bq m^{-3}.

https://doi.org/10.1017/RDC.2023.68 Published online by Cambridge University Press

Gaussian Plume Dispersion Model for $^{14}CO_2$ Activity Prediction

Using basic Gaussian plume dispersion model (GPM) (Equation [5]), $^{14}CO_2$ activity is calculated.

$$\chi(x,y,z) = \frac{Q}{2.\pi.u.\sigma_y.\sigma_z} * \exp\left(-\frac{y^2}{2.{\sigma_y}^2}\right) * \left[\exp\left(-\frac{(z-H)^2}{2.{\sigma_Z}^2}\right) + \exp\left(-\frac{(z+H)^2}{2.{\sigma_Z}^2}\right)\right] \quad (5)$$

For the above equations, the origin is at the base of the stack, and x-, y-, and z- axes are in the horizontal downwind, horizontal cross-wind and the vertical directions, respectively. The symbols used are: χ (x,y,z) = mean effective $^{14}CO_2$ concentration Bq m^{-3} of the effluent at a point (x,y,z) in the plume; y = cross wind distance in (m) from the center line of the plume; z = height above ground in (m) where concentration is calculated; u = mean velocity in the x-direction (m s^{-1}) at stack height 100 m; H = the effective height of release (m), Q = $^{14}CO_2$ source strength in Bq s^{-1} which is emitted in CO_2 gaseous form from stack; σ_y and σ_z in (m) = standard deviations of the assumed normal distribution at distance x in the cross-wind and vertical directions respectively which depends upon the stability category and downwind distance between source and receptor, the dispersion parameters are used which is based on Pasquill–Guifford scheme (Eimutis and Konicek 1972). Meteorological parameters such as wind speed, wind direction, ambient temperature, relative humidity, atmospheric pressure, solar radiation, and rainfall are measured at micrometeorological laboratory of Environmental Survey Laboratory of Kakrapar Gujarat Site. As GPM is dependent upon source strength and meteorological parameter, $^{14}CO_2$ activity of NPP stack, micro-meteorological monitoring of wind speed, wind direction and atmospheric stability data were used for the prediction of $^{14}CO_2$ activity in the air samples collected at 1.6 km towards NNE downwind sector.

Estimation of Atmospheric Dilution Factor

The atmospheric dilution factors are important indicators of diffusive properties of the site. They are useful for estimating the annual averaged concentration distribution of gaseous effluents released from nuclear facilities. There are two ways to estimate atmospheric dilution factors. One way is routinely measured hourly meteorological data are used in the preparation of diffusion climatology of the site which in turn is used to estimate the dilution factors. Another way is to experimentally evaluate the dilution factor by taking the ratio of source/release point measuring contaminant activity to receptor of interest measuring contaminant activity. An attempt was made to evaluate the site specific atmospheric dilution by measuring $^{14}CO_2$ activity at NPP stack and at 1.6 km towards NNE downwind sector. Dilution factor of $^{14}CO_2$ at 1.6 km depends upon two important parameters: (a) source strength and (b) meteorological parameters.

RESULTS AND DISCUSSION

$^{14}CO_2$ Activity in Air Samples

$^{14}CO_2$ activity in air along with meteorological parameters is tabulated in Table 1. $^{14}CO_2$ activity was found at the range of (0.10 ± 0.01) – (0.18 ± 0.01) TBq (GW_e.year) $^{-1}$, with mean value 0.12 ± 0.01 TBq (GW_e.year)$^{-1}$ at NPP stack which is comparable with other PHWR type reactor (Bharath et al. 2022 and Sohn et al. 2012). Bharath et al. (2022) studied the ^{14}C activity at Indian PHWR, Kaiga Generating Station (KGS) during the year 2017–2020 and reported the normalized ^{14}C emission with geometric mean value of 0.12 TBq (GW_e.year)$^{-1}$. Bharath et al. (2022) also reported that the ^{14}C released in oxide form (CO_2) and less than

https://doi.org/10.1017/RDC.2023.68 Published online by Cambridge University Press

Table 1 $^{14}CO_2$ activity in air samples with associated meteorological parameters.

Parameter	Min	Max	AM	SD	GM	GSD	25th perc.	75th perc.
Wind speed (m s^{-1})	0.4	7.8	2.9	1.8	2.4	1.9	1.6	3.9
Ambient temp. (°C)	22.1	32.1	27.0	2.4	26.9	1.1	25.2	28.6
Atm. pressure (mbar)	991	1003	999	3	999	1	998	1001
RH (%)	61	99	84	10	84	1	78	92
Solar radiation (Cal cm^{-2})	0.7	75.0	32.6	19.8	25.0	2.3	14.6	48.6
Inter angle (degree)	1.0	160.0	61.5	37.9	46.7	2.4	36.0	89.5
$^{14}CO_2$ activity in Fence post (Bq m^{-3})*	≤0.04	0.13	0.08	0.02	0.08	1.30	0.07	0.09
Dilution factor (s m^{-3})	4.6E-05	2.1E-04	1.3E-04	3.1E-05	1.2E-04	1.35	1.0E-04	1.4E-04

*Number of samples = 72.

Table 2 Comparison of $^{14}CO_2$ activity in air samples with worldwide data.

Location	Sampling duration	Distance from stack (km)	$^{14}CO_2$ activity (Bq m^{-3})	Reference
Kakrapar Gujarat Site, India	2021	1.6	≤0.04–0.13	Present study
TarapurMaharastra Site, India	2014–2018	1.8–3.9	<0.05–0.125	Baburajan et al. (2020)
Wolsong site, South Korea	1997–1998	1–2	0.05–0.095	Kim et al. (2000)
Krsko site, Slovenia	2008	Within site area	0.064–0.12	Breznika et al. (2008)
La Hague Nuclear Reprocessing Plant, France	1997–1999	4–6	0.08–0.18	Fontugne et al. (2004)
Qinshan site, China	2011	0.5–5	0.046–0.052	Wang et al. (2014)
Angra site, Brazil	2002–2005	0.4–3.0	0.054–0.060	Dias et al. (2009)
Bohunice site, Slovakia	2001–2005	5	0.044	Povinec et al. (2008)

1.27 % of total release in reduced form (CH_4). Sohn et al. (2012) estimated the ^{14}C inventory of CANDU PHWR type reactor at Wolsong Nuclear Power Plant and normalized measured emission observed to be 0.14 and 0.16 TBq $(GW_e.year)^{-1}$ during the year 2001 and 2000, respectively. To detect lower $^{14}CO_2$ activity in environmental samples, counting time increases and MDL of ^{14}C in air Bq m^{-3} at a confidence level of 99.7% is 0.04 Bq m^{-3}. $^{14}CO_2$ activity was found to be in the range of ≤0.04 – (0.13±0.033) Bq m^{-3}, with mean value 0.08 ± 0.02 Bq m^{-3} at site boundary (1.6 km towards NNE) and is comparable with worldwide values as shown in Table 2. $^{14}CO_2$ environmental activity data with similar sampling distance are comparable with other PHWRs type reactors: Tarapur Maharashtra Site, India, and Wolsong site, South Korea, as reported in Table 2. One data point was found to be BDL (≤0.04 Bq m^{-3}) at site boundary

https://doi.org/10.1017/RDC.2023.68 Published online by Cambridge University Press

Table 3 Statistical correlation between dilution factor (s m^{-3}) of $^{14}CO_2$ with meteorological parameters.

Parameter	Inter-angle (degree)	Rainfall (mm)	Stability class	Relative humidity (%)	Wind speed (m s^{-1})	Ambient temp. (K)
r	–0.86	–0.28	–0.03	–0.18	–0.06	0.04
p level (two-tailed)	<0.00001	0.01	0.80	0.13	0.62	0.74

and all other detectable values are comparatively very low as compared to exhaust air of KAPS-1&2 stack. As a part of the reference sampling for the determination of $^{14}CO_2$ activity in air, the sampling was carried out at 30–35 km from Kakrapar Gujarat nuclear power plant site, and $^{14}CO_2$ activity was ≤0.04 Bq m^{-3}. Factors affecting $^{14}CO_2$ activity measured at 1.6 km fence post are source strength and meteorological parameter (inter-angle and rainfall), other meteorological parameters do not have much influence in dilution of $^{14}CO_2$ activity at 1.6 km. It is observed that as the $^{14}CO_2$ activity released from NPP stack (source strength) increases, $^{14}CO_2$ activity measured at 1.6 km fence post increases and a positive statistically significant correlation is observed (correlation coefficient (r): 0.42 and p value = 0.00024 (two-tailed).

Correlation of Observed $^{14}CO_2$ Activity in the Air Samples with the Predicted Activity

$^{14}CO_2$ activity in the air samples were predicted using Gaussian plume dispersion model (GPM) for 72 different sampling events. Predicted activity was varying from 10^{-8} - 0.0025 Bq m^{-3} at 1.6 km for all the 72 sampling events. There is a large variation of predicted $^{14}CO_2$ activity. GPM calculation is highly dependent upon inter angle between plume direction and the fixed sampling location. As the inter angle is larger, the $^{14}CO_2$ activity decreases significantly. When the plume direction is towards NNE sector, then predicted $^{14}CO_2$ activity calculated using GPM was 0.001–0.0025 Bq m^{-3} and is lower than the measured activity ≤0.04–0.13 Bq m^{-3}. Dias et al. (2009) and Varga et al. (2020) reported that the dilution and dispersion of $^{14}CO_2$ do not follow GPM. The main reason behind this is CO_2 density is larger than that of air density (Molnár et al. 2007) and GPM equation does not account density explicitly. Out of 72 sampling events, in 37 events wind speeds are less than 2.5 m s^{-1} at 30 m height, and at 25 events wind speeds are 2.5–5 m s^{-1}. This indicates low wind speed is observed in our region during the sampling event and the model does not give precise results during low wind speeds.

Estimation of Dilution Factor for $^{14}CO_2$ Activity

Dilution factor of $^{14}CO_2$ at 1.6 km depends upon two important parameters: (a) source strength and (b) meteorological parameters. Based on the $^{14}CO_2$ activity measured at two different locations (NPP stack and at 1.6 km), dilution factor (s m^{-3}) for $^{14}CO_2$ was evaluated by taking the ratio of $^{14}CO_2$ activity at 1.6 km (Bq m^{-3}) to $^{14}CO_2$ emission from NPP stack (Bq s^{-1}). The dilution factor for $^{14}CO_2$ was found to be in the range of 4.6E-05 to 21E-05 s m^{-3} as shown in Table 1. In Table 3, $p<0.05$ was observed for only two parameters: inter-angle and rainfall, which were statistically significant. Negative correlation was observed in inter-angle and rainfall. This implies the dilution factor increases, i.e., ambient activity increases with decreasing inter-angle and rainfall. Other parameters such as stability class, RH, WS, and AT were not showing any statistical significance. Variation of $^{14}CO_2$ dilution factor at 1.6 km

https://doi.org/10.1017/RDC.2023.68 Published online by Cambridge University Press

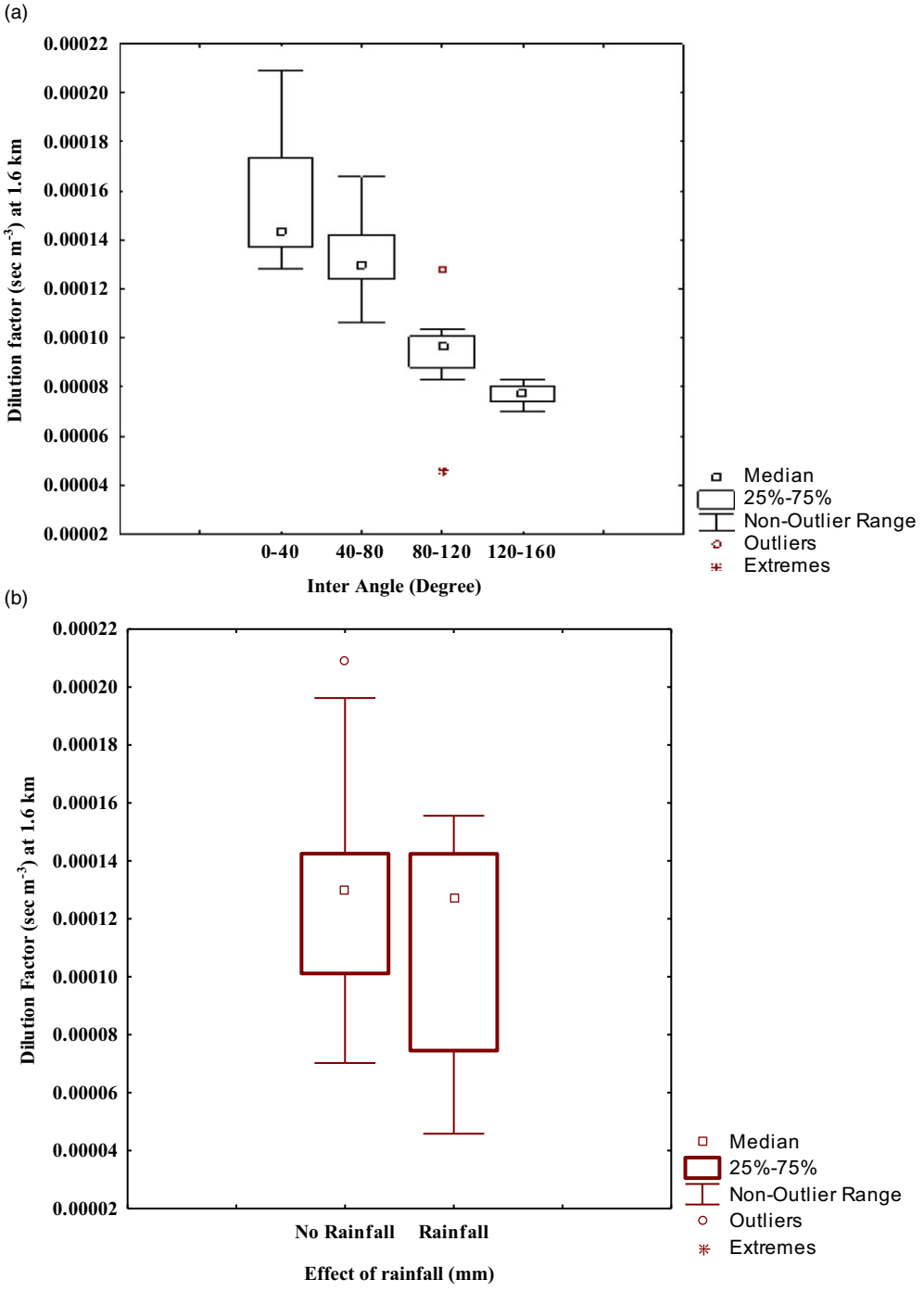

Figure 4 Variation of $^{14}CO_2$ dilution factor with inter angle (a) and rainfall (b).

https://doi.org/10.1017/RDC.2023.68 Published online by Cambridge University Press

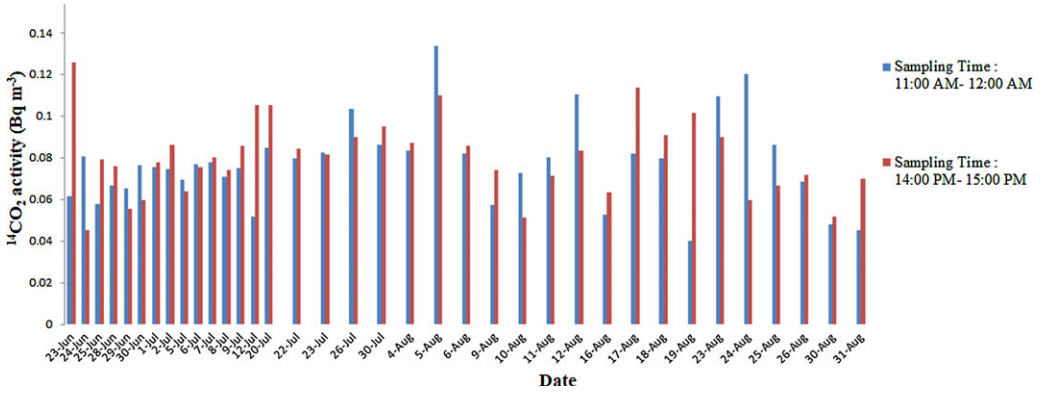

Figure 5 Variation of $^{14}CO_2$ activity (Bq m^{-3}) in air samples at 1.6 km, NNE sector with sampling date and time wise (11 AM–12 AM and 14 PM–15 PM), year: 2021.

(NNE Sector) with (a) Inter angle (degree) between plume direction and fixed sampling location: 1.6 km (NNE Sector); (b) presence/absence of rainfall (mm) are represented through Box and whisker plot (Figure 4 a–b). In Figure 4a, at inter-angle 80–120 degree, an asterisk indicates lowest observed dilution factor 4.6E-05 s m^{-3} due to highest rainfall (7 mm) which occurred during that sampling period. During the study period, sampling was carried out on twelve different rainy days (0.5–7 mm hr^{-1}) and $^{14}CO_2$ activity in air sample was significantly lower during the rainy days. The reduction of $^{14}CO_2$ activity in air samples is due to the washout of $^{14}CO_2$ in rain water. Contribution of rainfall in $^{14}CO_2$ dilution factor played an important role and was also reported by Pathakoti et al. (2018). When the plume direction was towards the receptor of interest, $^{14}CO_2$ activity is higher. The highest dilution factor of 21E-05 s m^{-3} was observed when inter-angle was smallest (1 degree), which can also be visualized from Figure 4a. From Figure 5, one can visualize that most of the $^{14}CO_2$ activity are nearly 0.08 Bq m^{-3}. Out of 72 sampling events, activity data are more than 0.10 Bq m^{-3} in 11 cases. In those 11 cases, plume direction was towards our sampling location, i.e., NNE sector (smaller inter-angle) in 7 cases and in remaining 3 cases, NPP stack (onsite) $^{14}CO_2$ source strength was little higher from average observed release 0.12 TBq (GW$_e$.year)$^{-1}$. Therefore, $^{14}CO_2$ activity in environmental air samples is mainly dependent upon plume direction.

CONCLUSIONS

Studies on $^{14}CO_2$ activity in air samples were carried out at Kakrapar Gujarat site, India where pressurized heavy water nuclear reactors have operated since 1993. $^{14}CO_2$ activity in air at NPP stack (onsite) and at meteorology laboratory of ESL (at 1.6 km from reactor) are observed to be (0.10 ± 0.01) – (0.18 ± 0.01) TBq (GW$_e$.year) $^{-1}$, with mean value 0.12 TBq (GW$_e$.year)$^{-1}$ and ≤0.04 – (0.13 ± 0.033) Bq m^{-3}, with mean value 0.08 ± 0.02 Bq m^{-3}, respectively. Based on the activity measurement, the dilution factor for $^{14}CO_2$ in air was evaluated at 1.6 km and was found to be in the range of 4.6E-05 to 21E-05 s m^{-3}. The minimum dilution factor is observed on rainy days due to washout of $^{14}CO_2$ activity from air. Inter angle (degree) between plume direction and fixed sampling location and rainfall (mm) are important influencing parameters for dilution factor of $^{14}CO_2$ in air. When the plume direction was towards the sampling

https://doi.org/10.1017/RDC.2023.68 Published online by Cambridge University Press

location, $^{14}CO_2$ activity was comparatively higher. $^{14}CO_2$ activity in air was reduced during rain events. The site-specific dilution factor estimation is an important input parameter used for the prediction of radionuclide distribution pattern at different locations.

REFERENCES

Baburajan A, Dalvi SS, Sudheendran V, Varakhedkar VK, Saradhi IV, Ravi PM, Karunakara N. 2020. Validation of a method for measurement of ^{14}C in air and its application for estimation of ^{14}C levels around Tarapur nuclear site. Journal of Radioanalytical and Nuclear Chemistry 324:551–559.

Bharath, Arya Krishnan K, D'Souza RS, Rashmi Nayak S, Dileep BN, Ravi PM, Mangavi SS, Salunke GS, Veerendra D, Karunakara N. 2022. Carbon-14 emission from the pressurized heavy water reactor nuclear power plant at Kaiga, India. Journal of Environmental Radioactivity 255:107006.

Breznika B, Volčanšeka A, Zlata Božnar M, Mlakar P, Krajcar Bronić I, Obelić B. 2008. Verification of the dispersion model by airborne ^{14}C. In: 12th international congress of International Radiation Protection Association (IRPA-12) at Buenos Aires, Argentina.

Davis W Jr. 1977. Carbon-14 production in nuclear reactors. No.ORNL/NUREG/TM–12. Oak Ridge National Lab.

Dias CM, Stenström K, Bacelar Leão IL, Santos RV, Nícoli IG, Skog G, Ekström P, da Silveira Corrêa R. 2009. $^{14}CO_2$ dispersion around two PWR nuclear power plants in Brazil. Journal of Environmental Radioactivity 100:574–580.

Eimutis EC, Konicek MG. 1972. Derivations of continuous functions for the lateral and vertical atmospheric dispersion co-efficients. Atmospheric Environment 1967:859–863.

Fontugne M, Maro D, Baron Y, Hatté C, Herbert D, Douville E. 2004. ^{14}C sources and distribution in the vicinity of La Hague nuclear reprocessing plant: part-I terrestrial environment. Radiocarbon 46(2):827–830.

Graven HD, Gruber N. 2011. Continental-scale enrichment of atmospheric $^{14}CO_2$ from the nuclear power industry: potential impact on the estimation of fossil fuel-derived CO_2. Atmospheric Chemistry and Physics 11(23):12339–12349.

Huang YJ, Guo GY, Wu LS, Zhang B, Chen CF, Zhang HY, Qin HJ, Shang-Guan ZH. 2015. An analytical method for ^{14}C in environmental water based on a wet oxidation process. Journal of Environmental Radioactivity 142:1–8.

IAEA. 2004. Management of waste containing tritium and carbon-14. Technical Reports Series No. 421.

IAEA-TECDOC-1401. 2004. Quantifying uncertainity in nuclear analytical measurements.

Joshi ML, Ramamirtham B, Soman SD. 1987. Measurement of ^{14}C emission rates from a pressurised heavy water reactor. Health Physics 52:787–791.

Kim CK, Lee SK, Rho BH, Lee YG. 2000. Environmental distribution and behaviour of ^{3}H and ^{14}C around Wolsong Nuclear Power Plant. Health Physics 78(6):693–699.

Kutschera W. 2013. Applications of accelerator mass spectrometry. International Journal of Mass Spectrometry 349–350:203–218.

Lassey K, Etheridge DM, Lowe DC, Smith AM, Ferretti DF. 2007a. Centennial evolution of the atmospheric methane budget: what do the carbon isotopes tell us? Atmospheric Chemistry and Physics 7(8):2119–2139.

Lassey K, Lowe DC, Smith AM. 2007b. The atmospheric cycling of radiomethane and the "fossil fraction" of the methane source. Atmospheric Chemistry and Physics 7(8):2141–2149.

Pathakoti M, Gaddamidi S, Gharai B, Sudhakaran Syamala P, Venkata Narasimha Rao P, Choudhury SB, Venkata Raghavendra K, Dadhwal VK. 2018. Influence of meteorological parameters on atmospheric CO_2 at Bharati, the Indian Antarctic research station. Polar Research 37(1):1442072.

Molnár M, Bujtás T, Svingoré, Futó I, Světlík I. 2007. Monitoring of atmospheric excess ^{14}C around Paks nuclear power plant, Hungary. Radiocarbon 49:1031–1043.

Peterson SR, Davis PA, Rao RR. 1997. Modeling doses from tritium and ^{14}C in the environment, RC-1951. Atomic Energy of Canada Limited (AECL).

Povinec PP, Sivo A, Simon J, Holý K, Chudý M, Richtáriková M, Morávek J. 2008. Impact of the Bohunice Nuclear Power Plant on atmospheric radiocarbon. Applied Radiation and Isotopes 66:1686–1690.

Povinec PP, Chudy M, Sivo A, Simon J, Holy K, Richtarikova M. et al. 2009. Forty years of atmospheric radiocarbon monitoring around Bohunice nuclear power plant, Slovakia. Journal of Environmental Radioactivity 100:125–130.

Robertson JAL. 1978. The CANDU reactor system: an appropriate technology. Science 199(4329): 657–664.

Sohn W, Kang DW, Kim WS. 2012. An estimate of carbon-14 inventory at wolsong nuclear power plant in the republic of Korea. Journal of Nuclear Science and Technology 40(8):604–613.

Stenström K, Skog G, Thornberg C, Erlandsson B, Hellborg R, Mattsson S, Persson P. 1998. ^{14}C levels in the vicinity of two Swedish Nuclear

https://doi.org/10.1017/RDC.2023.68 Published online by Cambridge University Press

Power Plants and at two "clean-air"sites in southernmost Sweden. Radiocarbon 40:433–438.
UNSCEAR. 2000. United Nations Scientific Committee on the Effects of Atomic Radiation. Sources and effects of ionizing radiation. Report to the General Assembly with scientific annexes. Vol I.
Varga T, Orsovszki G, Major I, Veres M, Bujtás T, Végh G, Manga L, Jull AJT, Palcsu L, Molnár M. 2020. Advanced atmospheric ^{14}C monitoring around the Paks Nuclear Power Plant, Hungary. Journal of Environmental Radioactivity 213:106138.
Vokal B, Kobal I. 1997. Radiocarbon releases at the krsko nuclear power. Radiocarbon 39:285–292.
Wang Z, Hu D, Xu H, Guo Q. 2014. ^{14}C distribution in atmospheric and aquatic environments around Qinshan nuclear power plant, China. Radiocarbon 56(3):1107–1114.

https://doi.org/10.1017/RDC.2023.68 Published online by Cambridge University Press